AIR POLLUTION CONFERENCE BRAZIL
CMAS SOUTH AMERICA
COMMUNITY MODELING AND ANALYSIS SYSTEM

AEROSOL OPTICAL PROPERTIES IN THE ATMOSPHERE OF NATAL/BRAZIL BY AN AERONET NETWORK SUN-PHOTOMETER

Daniel Camilo Fortunato dos Santos Oliveira[1*], Judith Johanna Hoelzemann[1], Eduardo Landulfo[2], Lucas Alados-Arboledas[3], Juan Luis Guerrero-Rascado[3]

[1]*Federal University of Rio Grande do Norte, Department of Atmospheric and Climate Sciences (UFRN/DCAC), Natal, Brazil*

[2]*Institute of Energy and Nuclear Research (IPEN), Center for Laser and Applications, São Paulo, Brazil*

[3]*University of Granada (UGR), Andalusian Institute for Earth System Research (IISTA-CEAMA), Granada, Spain*

[*]*Corresponding author: danielcammilo@hotmail.com*

Abstract: The study of atmospheric aerosols contributes to the understanding of radiative forcing and global warming. In addition, aerosols may influence atmospheric chemistry, visibility, precipitation and human health. Since 2016, Natal (capital of Rio Grande do Norte, Brazil) has a Sun-photometer (CIMEL) of the RIMA-AERONET network that can identify the presence of biomass burning aerosols and desert dust from Africa. For this identification, it is aimed to characterize the optical properties of these aerosols present in the atmosphere of Natal. The level 1.5 data (version 3) provided by AERONET provide information on some aerosol characteristics such as Aerosol Optical Depth (AOD), Ångström Exponent (α), Single Scattering Albedo (SSA), Asymmetry Factor (g), Complex Refractive Index (N) and Volume Size Distribution (VSD). The analysis period was from August 2017 to March 2018. Aerosols were classified according to global climatologies and their optical properties were described. In addition, backward trajectories were modeled using the HYSPLIT model (version 4.8) to identify the predominant air masses origins. Aerosols present in the atmospheric column of Natal showed monthly mean AOD (500 nm)in the range of 0.10 to 0.(representing ~40%), monthly means of α (440-670 nm)between 0.6 and 0.8 (representing 30%), bimodal VSD with dominant coarse mode, SSA (440 nm) about 0.80, real part around 1.500, imaginary part ranging from 0.0125 to 0.0437 and g above 0.74. The classification showed mixed (60.4%), marine (30.7%) and mineral dust (8.9%) aerosols. The backward trajectories identified that, in about 51% of the cases, are originated from Africa.

Keywords: *Sun-photometer, desert dust, AERONET, HYSPLIT.*

INTRODUCTION

One of the main components of the atmosphere are the aerosols. These atmospheric components can influence radiative forcing, global climate, visibility (Seinfeld and Pandis, 2016), human health (Fuzzi et al., 2015), cloud formation (Koren et al., 2008), precipitation, air quality (Orza and Perrone, 2015) and carbon cycle, modifying the land and ocean uptake of anthropogenic CO_2 (IPCC, 2018). Among the atmospheric aerosols, there is desert dust, focus of this study, is an important component in biogeochemical cycles (Abouchami et al., 2013) and fertilization of the Amazon rainforest and oceans, contributing with micro- and macro-nutrients (Kaufman et al., 2005; Kumar et al., 2014).

A detailed knowledge of their optical and microphysical properties and distributions, is required in studies on the Earth's climate and its temporal variations (Hamill et al., 2016). Consequently, this reduces the uncertainties about the impact of aerosols on climate (IPCC, 2013). Thus, there is a need of monitoring and studying both anthropogenic and natural aerosols. Among other techniques, the monitoring and observation of atmospheric aerosols can be performed by remote sensing. In the last decades, remote sensing networks were created worldwide to improve our knowledge on aerosols such as Global Atmospheric Watch (GAW), European Aerosol LIDAR Network (EARLINET), Latin American LIDAR Network (LALINET) and Aerosol Robotic Network (AERONET). The last one represents the efforts to reduce the uncertainties in the estimation of the radiative forcing of aerosols (Holben et al., 1998). Along the years, AERONET retrieving algorithm has evolved from the the Version 1 algorithm based on the inversion code of Dubovik and King (2000), to the Version 2 code developed by Holben et al. (2006), which improves the inversion products and, recently, the Version 3 algorithm, which provides quality cloud scanning and fully automatic instrument anomaly controls (Giles et al., 2019).

In order to study atmospheric aerosols, Natal (capital of Rio Grande do Norte (RN) in Brazil) has joined AERONET through RIMA (Red Ibérica de Medida fotométrica de Aerosoles) in 2016. Natal is located in a region where the long-range transport of mineral dust from the African continent occurs under strong influence of the trade winds during December, January and February, when the Intertropical Convergence Zone (ITCZ) is positioned further South (Talbot et al., 1990; Swap et al. 1992; Landulfo et al., 2016).

Some studies prove the presence of desert dust from the African continent in the atmosphere of southern hemisphere regions, such as Ascension Island (Smirnov et al., 2002), Amazon basin (Ben-

Ami et al., 2010; Baars et al., 2011) and eastern Brazil (Wang et al., 2016).These findings were possible due to the characteristics of the aerosols observed. It is important to accurately characterize the optical properties of representative types of ambient aerosol particles to assess its impact on the Earth's energy budget and climate change (Rizzo et al., 2013). Indeed, the aerosol features are needed to incorporate aerosol particles into global climate models and evaluate climate forcing effects produced by aerosols of different origin and composition (Perrone et al., 2005).

This paper focuses on the characterization of optical properties of the aerosols present in the atmosphere of Natal, making it a pioneer study at the region due to the use of a CIMEL Sun-photometer to obtain the optical properties of aerosols.

The paper has the following structure: the measurement site, the Methods section, which the instrumentation and methodology are described, Findings and Argument section, where the results for each optical property of aerosols are presented and discussed and, finally, the conclusions.

METHODS

Measurement site

Natal is the capital of Rio Grande do Norte (RN), one of the states of the Northeastern Region of Brazil (NRB) (Figure 1). It is a coastal city (05°47'42" S, 35°12'34" W, 30 m asl) and its climate is tropical with a rainy season that extends from Southern autumn to winter (Alvares et al., 2014) , with months of May to July with the highest rainfall. According to the National Institute of Meteorology, the average temperature is 26 °C, solar irradiation produces around 3,000 hours of sunshine per year and the average rainfall is 1465 mm/year.

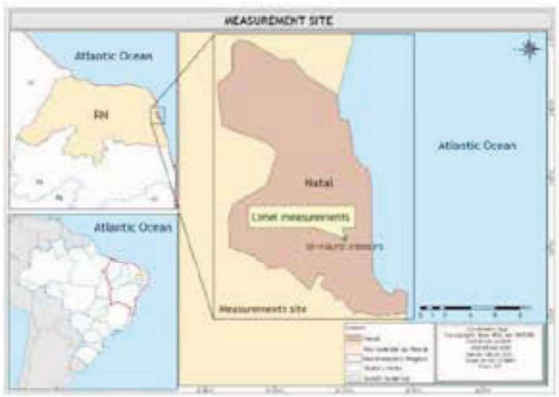

Figure 1. Location of the measurement site, Natal capital of Rio Grande do Norte (Brazil).

The ITCZ, Easterly Wave Disturbances (EWDs), Upper Tropospheric Cyclonic Vortex (UTCV) and sea-breeze circulation favor NRB precipitation (Cavalcanti et al., 2009) and, consequently, the precipitation in Natal. Another feature is that the evaporation of the sea forms a series of low clouds (cumulus and fractocumulus types) throughout the year (Motta, 2004).

Instrumentation

The instrument used for the measurements was the CIMEL Sun-photometer, standard model CE-318. It provides retrievals from direct Sun measurements of aerosol and water vapor content (940 nm), in addition to aerosol properties from inversion of spectral sky radiances (Holben et al., 1998). The CIMEL makes two protocols of measurements, either direct Sun or sky ones, both within several programmed sequences. The direct Sun measurements are made in eight spectral bands channels (between 340 nm and 1020 nm, being 440, 670, 870 and 940 nm the standard channels) and sky measurements are performed at 440, 670, 870 and 1020 nm in two sky observation sequences (almucantar and principal plane) to acquire aureole and sky radiances observations through a large range of scattering angles from the Sun through a constant aerosol profile to retrieve size distribution, phase function, and aerosol optical thickness (AOT) (Holben et al., 1998). See Holben et al. (1998) for more details.

Calculation of aerosol optical properties

Optical Aerosol Depth (AOD), Ångström Coefficient (α), Single Scattering Albedo (SSA), Asymmetry Factor (g), Complex Refractive Index (N) and Volume Size Distribution (VSD) were the optical properties used in the characterization of the aerosols in the atmospheric column of Natal.

In this study, the wavelength 440 nm was used for the optical properties VSD, SSA, N and g with AOD (440 nm) values > 0.4 (Holben et al., 1998; Prats et al., 2008) and the wavelength 500 nm was used for the calculation of AOD, provided by AERONET with accuracy of ~0.015 (Fuzzi et al., 2015), because the mineral dust absorbs significantly in the wavelengths blue and UV, due to the iron oxide impurities (Sokolik et al., 1999; Kaufman et al., 2002; Olmo et al., 2008; Valenzuela et al., 2010), with 500 nm being a well-used standard wavelength (O'Neill et al., 2000; O'Neill et al., 2001; Smirnov et al., 2002). Moreover, the 440 nm was insufficient due to the large amount of negative values and the few days with data for AOD. Therefore, the range of 440-670 nm was used for the α calculation. Currently, Natal makes its measurements with a second CIMEL (#752) and provides data at level 1.5, since the instrument has not been calibrated and therefore does not provide the level of quality assured (2.0) yet.

In January 2016, Natal joined the RIMA-AERONET network (the city's first CIMEL and the second in the NRB). It was brought to the Federal University of Rio Grande do Norte through a partnership between the Institute of Energy and Nuclear Research (IPEN-São Paulo), the Research Group on Atmospheric Chemistry Modeling and Observation (GP-MOQA,

UFRN) and the University of Granada (Spain). An analysis of the temporal evolution was made for AOD and α from August 2017 to March 2018 and for other properties until January 2018. On other hand, the aerosol typing was based on the main climatologies developed in AERONET (Eck et al., 1999; Holben et al., 2001; Smirnov et al., 2002). The optical depth data were at level 1.5 of the new version of AERONET (Version 3) as well as aerosol inversion data (VSD, SSA, N and g). However, inversion data is only available until January 2018, because, in order to have a good inversion, the sky must be free of clouds at a low Sun angle. This resulted in the number of days with inversion data to decrease.

HYSPLIT

The HYbrid Sigle-Particle Lagrangian Integrated Trajectory (HYSPLIT) can be used to attribute a type of aerosol to the origin of the air masses. According to (Toledano et al., 2009), when analyzing the back trajectories, the main assumption is that there is a link between the origin of the air mass and/or path and the aerosol observations at the receiving site. The back trajectories were calculated within 10 days and for each day that had available level 1.5 AERONET observations of (V 3), totaling 102 days with modeling and five back trajectories per day (500, 1500, 3000, 4000 and 6000 m agl). It was possible, then, to know how many back trajectories came from the African continent and from other origins.

FINDINGS AND ARGUMENT

Figure 2 shows the monthly average of AOD (500 nm) for almost every month and these values are close to those found by Smirnov et al. (2002) for coastal areas and continental seas (AOD (500 nm) > 0.12). February 2018 (~0.20) was the unique month whose average was above 0.15, probably due to the transport of dust from the African continent most present this month. AOD on the Natal atmosphere was mostly between 0.05 to 0.15 (~70%) and only 20% of the values are between 0.15 and 0.20. These values are attributed to the presence of marine aerosols (Knobelspiesse et al., 2004) and values between 0.20 and 0.50 to the desert aerosols (Holben et al., 2001). However, AOD (500 nm) < 0.20 can also be attributed to biomass-burning aerosols (Sena and Artaxo, 2015).

Figure 3 shows a subtle seasonality for the Southern hemisphere summer (averages between 0.6 and 0.8 from December 2017 to March 2018), the lowest monthly average was in September 2017 (0.38) and the maximum in March 2018 (0.76).

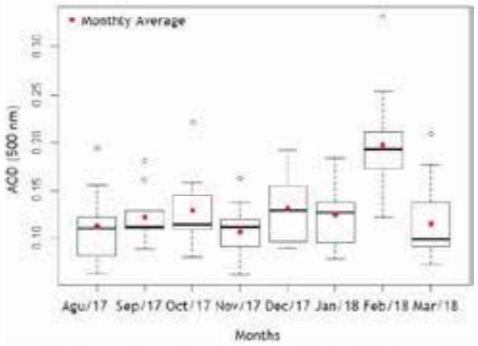

Figure 2. Boxplot of monthly AOD (500 nm) from August 2017 to March 2018. The base of the boxes represents the first quartile, the center lines represents the median, the top of the boxes represents the third quartile and the red points the monthly average.

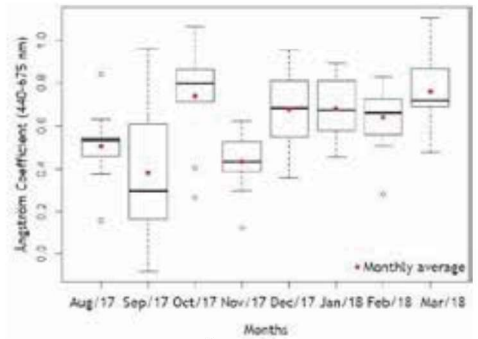

Figure 3. Boxplot of Ångström Coefficient (440-675 nm) from August 2017 to March 2018.

The high variability in September may be related to the contribution of biomass burning aerosol from the burning of sugarcane in the regions near Natal, but also may be related to low number of datapoints. Close values (around 0.6-0.7) were found in Cuiabá (Brazil) (Holben et al., 2001). More than 60% of the α (440-670 nm) values were between 0.4 and 0.8 and more than 20% were between 0.8 and 1.0. The results over Natal resemble those of Smirnov et al. (2002) for Ascension Island with dominant values typically below 1.0, under scenarios with predominance of coarse particles.

Figure 4 shows that the aerosol over Natal is bimodal with a dominant volume in coarse mode for the months of December 2017 (0.036 $\mu m^3/\mu m^2$), September 2017 (0.034 $\mu m^3/\mu m^2$) and November 2017 (0.028 $\mu m^3/\mu m^2$) with the largest distributions. The fine mode stands out in the months of December 2017 (0.008), October 2017 (0.007 $\mu m^3/\mu m^2$) and January 2018 (0.005 $\mu m^3/\mu m^2$).

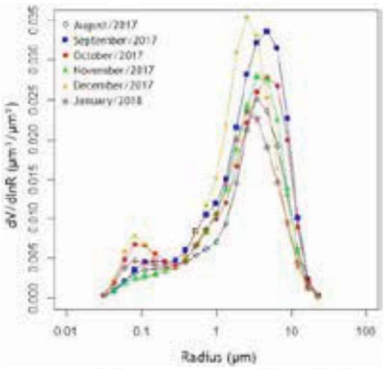

Figure 4. Monthly average of the Volume Size Distribution (µm³/µm²) from August 2017 to January 2018.

The fine mode is probably related to fuel-burning or biomass-burning aerosols. However, there was no discernible relationship between the aerosols of fine mode and the months under review, which leads to reinforcing the need for a more accurate statistic. The radius that separates coarse mode and fine mode is 0.33 µm which was a value close to those found by Smirnov et al. (2002) on five islands around the globe (0.40 µm) and by Taylor et al. (2015) for the dust cluster (0.35 µm).

Aerosol microphysical properties

Table 1 reports the aerosol microphysical properties found in this period. SSA (440 nm) remains around 0.80 for the period of observations. This result is close to what was found by Dubovik et al. (2002) for biomass burning in African Savannah (Zambia - 0.88 ± 0.015) and by Prats et al. (2008) for a range of 0.82 to 0.97 in characteristic of desert dust (Huelva - Spain).

The real part of N remains around 1.500 with the lowest value in December 2017 (1.444 ±0.05) and the imaginary part is very variable over the measurement period, with a monthly maximum in August 2017 (0.0437 ±0.03) and the minimum in September 2017 (0.0125 ±0.01). The observations of the real and imaginary part of complex refractive index are similar to those found by Dubovik et al. (2002) for mixed and industrial urban aerosol in Greenbelt (USA) (1.47 ±0.03; 0.014 ±0.0006), for biomass burning in the Brazilian Cerrado (1,52 ±0.01; 0.015 ±0.004) and the African Savannah (Zambia) (1.51 ±0.01; 0.021 ±0.004), for desert dust and ocean aerosol in Bahrian (Persian Gulf), Solar (Saudi Arabia) and Cape Verde (1,55 ±0.03, 1.56 ±0.03 and 1.48 ±0.05 respectively). However, Perrone et al. (2005) classified the days with values of 1.46 ± 0.09 and 1.50 ± 0.07 (real part) as urban industrial aerosols in Lecce (Italy).

The asymmetry factor (g) also did not change significantly over the period, with values above 0.74, whose maximum occurs in November 2017 (0.78 ±0.02) and the lowest occurs in October 2017 (0.75 ±0.06). These values agree with those of Dubovik et al. (2002) for desert dust and oceanic aerosol found in Cape Verde and Lanai, Hawaii, (0.73 ± 0.04, 0.75 ± 0.04, respectively), as well as Taylor et al. (2015) who found values of g = 0.74 for mineral dust.

Aerosol typing

The aerosol classification in Natal atmosphere (Figure 5) shows a mixture aerosol between mineral dust and marine aerosol (60.4%), marine aerosol (30.7%) and mineral dust (8.9%) based on climatologies of Holben et al. (2001) and Smirnov et al. (2002).

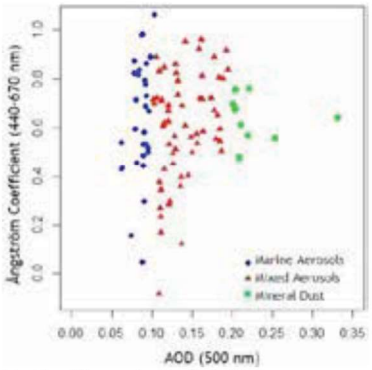

Figure 5. Scatter plot of daily averages of AOD (500 nm) vs. Ångström Coefficient (440-675 nm). The colors indicate the aerosol type.

The high percentage of mixed aerosols is due to the difficulty in distinguishing sea salt aerosols from those of dust, since both are associated with low Ångström exponents (Holben et al., 2001), having characteristics of both. The predominance of aerosols classified as mineral dust occurred in February 2018, possibly due to the ITCZ most displaced to the South in this period. A summary of the classification is shown in Table 2. These data are compatible with those used by Knobelspiesse et al. (2004) for AOD (50 nm) in North America (dust: 0.17, marine: 0.08) for the Pacific (maritime: 0.09) and for South Asia whose values for marine aerosol were in the range of mixed aerosol (0.14).

Origin of air masses

The Figure 6 shows the number of modeled back trajectories arriving from the African continent in Natal (261) and the quantity arriving from other regions (249). The amount of trajectories coming from the African continent is around 1500 to 4000 m above ground level, with the majority at 3000 m (70), validating the results found in previous studies (Swap et al., 1992; Holben et al. 2001; Toledano et al., 2009; Bem-Ami et al., 2010; Kumar et al., 2014; Orza and Perrone, 2015; Landulfo et al., 2016; Wang et al., 2016) for transatlantic air masses at 3000 m high.

Table 1. Monthly average and standard deviation for Single Scattering Albedo (SSA), Complex Refractive Index (real part and imaginary part) and Asymmetry Factor (g) at 440 nm from August 2017 to January 2018.

Aerosol property (440 nm)	August 2017	September 2017	October 2017	November 2017	December 2017	January 2018
SSA	0.75 ±0.10	0.86 ±0.05	0.81 ±0.05	0.81 ±0.08	0.83 ±0.10	0.77 ±0.07
Real *part* (N)	1.519 ±0.07	1.517 ±0.04	1.501 ±0.04	1.506 ±0.01	1.444 ±0.05	1.512 ±0.08
Imaginary part (N)	0.0437 ±0.03	0.0125 ±0.01	0.0231 ±0.01	0.0152 ±0.009	0.0153 ±0.02	0.0315 ±0.03
g	0.77 ±0.04	0.77 ±0.04	0.75 ±0.04	0.78 ±0.02	0.76 ±0.02	0.75 ±0.06

Reference: Oliveira (2019).

Table 2. Mean AOD (500 nm), standard deviation of AOD (σ_{AOD}), mean of α (440-670 nm), standard deviation of α (σ_{α}) for their respective classifications.

AOD (500 nm)	$\sigma_{AOD\ (500\ nm)}$	α (440-670 nm)	$\sigma_{\alpha\ (440-670\ nm)}$	Classification
0.09	0.01	0.65	0.25	Marine Aerosol
0.14	0.03	0.61	0.22	Mixed Aerosol
0.23	0.04	0.64	0.09	Mineral Dust

Reference: Oliveira (2019)

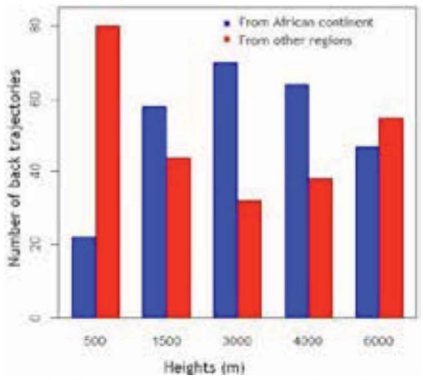

Figure 6. Bar graph for the back trajectories from Africa (blue color) and from other directions (red color) in five different height levels from August 2017 to March 2018.

CONCLUSIONS

For the first time it was possible to characterize the aerosol optical and microphysical properties present in the atmospheric column of Natal by a CIMEL Sun-photometer of AERONET.

The AOD, α, VSD, SSA, N and g showed predominant characteristics of desert dust and marine aerosols. Thus, the coarse mode was predominant, with a radius of 0.33 μm between modes. The classification of aerosols confirmed the predominance indicated by the optical properties (marine, dust and mixed aerosols), having February 2018 the highest number of days classified as mineral dust. In addition, the back trajectory modeling by HYSPLIT identified that half of them originated in the African continent (51%), especially at 3000 m agl (70 trajectories).

This study is the initial step to (i) generate a future climatology of aerosols properties for Natal; (ii) new studies with other aerosol properties (phase function, geometric radius, effective radius and others); (iii) future studies linking optical properties and chemical composition of aerosols; and (iv) other studies relating local sources of aerosols and the characteristics provided by the CIMEL Sun-photometer.

REFERENCES

ABOUCHAMI, W. et al. "Geochemical and isotopic characterization of the Bodélé Depression dust source and implications for transatlantic dust transport to the Amazon Basin." Earth and Planetary Science Letters 380 (2013): 112-123. doi: 10.1016/j.epsl.2013.08.028.

ALVARES, C. A. et al. "Köppen's climate classification map for Brazil." Meteorologische Zeitschrift 22 (2014): 711-728. doi: 10.1127/0941-2948/2013/0507.

BAARS, H. et al. "Further evidence for significant smoke transport from Africa to Amazonia." Geophysical Research Letters 38 (2011): p. 1-6. doi: 10.1029/2011GL049200.

BEM-AMI, Y. et al. "Transport of North African dust from the Bodélé depression to the Amazon Basin: a case study." Atmospheric Chemistry and Physics 10 (2010): 7533-7544, 2010. doi: 10.5194/acp-10-7533-2010.

CAVALCANTI, I. F. A. et al. Tempo e Clima no Brasil. São Paulo: Oficina de Textos: 2009.

DUBOVIK, O. and KING, M. D. "A flexible inversion algorithm for retrieval of aerosol optical properties from Sun and sky radiance measurements." Journal of Geophysical Research 105 (2000): 20673-20696. doi: 0148-0227/00/2000jd900282.

DUBOVIK, O. et al. "Variability of Absorption and Optical Properties of Key Aerosol Types Observed in Worldwide Locations." Journal of the Atmospheric Sciences 59 (2002): 590-608. doi: 10.1175/1520-0469(2002)059<0590:VOAAOP>2.0.CO;2.

ECK, T. F. et al. "Wavelength dependence of the optical depth of biomass burning, urban, and desert dust aerosol." Journal of Geophysical Research 104 (1999): 31333-31349. doi: 0148-0227/99/1999J D900923.

FUZZI, S. et al. "Particulate matter, air quality and climate: lessons learned and future needs." Atmospheric Chemistry and Physics 10 (2015): 7533-7544. doi: 10.5194 /acp-15-8217-2015.

GILES, D. M. et al. "Advancements in the Aerosol Robotic Network (AERONET) Version 3 Database - Automated Near Real-Time Quality Control Algorithm with Improved Cloud Screening for Sun Photometer Aerosol Optical Depth (AOD)

Measurements." Atmospheric Measurement Techniques 12 (2019) 169-209. doi: 10.5194/amt-12-169-2019.
HAMILL, P. et al. "An AERONET-based aerosol classification using the Mahalanobis distance." Atmospheric Environment 140 (2016): 213-233. doi: 10.1016/j.atmosenv.2016.06.002.
HOLBEN, B. N. et al. "AERONET-A Federated Instrument Network and Data Archive for Aerosol Characterization." Remote Sensing of Environment 66 (1998): 1-16. doi: 10.1016/S0034-4257(98)00031-5.
HOLBEN, B. N. et al. "An emerging ground-based aerosol climatology: Aerosol optical depth from AERONET." Journal of Geophysical Research 106 (2001):12067-12097. doi: 0148-0227/01/2001JD 900014.
HOLBEN, B. N. et al. "AERONET's Version 2.0 quality assurance criteria." Remote Sensing of the Atmosphere and Clouds 6408 (2006): 2006. doi: 10.1117/12.706524.
INSTITUTO NACIONAL DE METEOROLOGIA. Available in: <http://www.inmet.gov.br/portal/index.php?r=home2/index>.
INTERGOVERNMENTAL PANEL ON CLIMATE CHANGE. Climate Change 2013: The Physical Science Basis. IPCC: Cambridge University Press, New York, 2013.
INTERGOVERNMENTAL PANEL ON CLIMATE CHANGE. SPECIAL REPORT: Global Warming of 1.5 °C. IPCC: Cambridge University Press, New York, 2018.
KAUFMAN, Y. J. et al. "A satellite view of aerosol in the climate system." Nature Publishing Group 419 (2002): 215-223. doi: 10.1038/nature01091.
KAUFMAN, Y. J. et al. "Dust transport and deposition observed from the Terra-Moderate Resolution Imaging Spectroradiometer (MODIS) spacecraft over the Atlantic Ocean." Journal of Geophysical Research 110 (2005): 1-16. doi: 10.1029/2003JD004436.
KNOBELSPIESSE, K. D. et al. "Maritime aerosol optical thickness measured by handheld sun photometers." Remote Sensing of Environment 93 (2004): 87-106. doi: 10.1016/j.rse.2004.06.018
KOREN, I. et al. "Smoke Invigoration Versus Inhibition of Clouds over the Amazon." Science 321 (2008): 946-949. doi: 10.1126/science.1159185.
KUMAR, A. et al. "A radiogenic isotope tracer study of transatlantic dust transport from Africa to the Caribbean." Atmospheric Environment 82 (2014): 130-143. doi: 10.1016/j.atmosenv.2013.10.021.
LANDULFO, E. et al. "DUSTER Lidar: Transatlantic transport of aerosol particles from the Sahara and other sources: first results from the recently installed Lidar and sunphotometer in Natal/Brazil." Proceedings of SPIE, the International Society for Optical Engineering 10006 (2016): p. 1-9. doi: 10.1117/12.2241386.
MOTTA, A. G. O CLIMA DE NATAL. São José dos Campos: Instituto Nacional de Pesquisas Espaciais, 2004.
OLMO, F. J. et al. "Aerosol optical properties assessed by an inversion method using the solar principal plane for non-spherical particles." Journal of Quantitative Spectroscopy & Radiative Transfer 109 (2008): 1504-1516. doi: 10.1016/j.jqsrt.2007.12.019.
O'NEILL, N. T. et al. "The lognormal distribution as a reference for reporting aerosol optical depth statistics; Empirical tests using multi-year, multi-site AERONET sunphotometer data." Geophysical Research Letter 27 (2000): 3333-3336. doi: 0094-8276/00/2000GL011581.
O'NEILL, N. T. et al. "Modified Ångström exponent for the characterization of submicrometer aerossol." Applied Optics 40 (2001): 2368-2375. doi: 0003-6935y01y152368-08.
ORZA, J. A. G. and Perrone, M. R. "Trends in the aerosol load properties over south eastern Italy." IOP Conference Series: Earth and Environmental Science 28 (2015): 1-10. doi:10.1088/1755-1315/28/1/012011.
PERRONE, M. R. et al. "Aerosol load characterization over South-East Italy for one year of AERONET sun-photometer measurements." Atmospheric Research 75 (2005):111-133. doi: 10.1016/j.atmosres.2004.12.003.
PRATS, N. et al. "Columnar aerosol optical properties during "El Arenosillo 2004 summer campaign"." Atmospheric Environment 42 (2008): 2643-2653. doi: 10.1016/j.atmosenv.2007.07.041.
RIZZO, L. V. et al. "Long term measurements of aerosol optical properties at a primary forest site in Amazonia." Atmospheric Chemistry and Physics 13 (2013): 2391-2413. doi: 10.5194/acp-13-2391-2013.
SENA, E. T. and ARTAXO, P. "A novel methodology for large-scale daily assessment of the direct radiative forcing of smoke aerosols." Atmospheric Chemistry and Physics 15 (2015): 5471-5483. doi:10.5194/acp-15-5471-2015.
SEINFELD, J. H. and PANDIS, S. N. Atmospheric chemistry and physics: from air pollution to climate change. New Jersey: John Wiley & Sons, 2016.
SMIRNOV, A. et al. "Optical Properties of Atmospheric Aerosol in Maritime Environments." Journal of the Atmospheric Sciences 59 (2002): 501-523. doi: 10.1175/1520-0469(2002)059<0501:OPOAAI>2.0.CO;2.
SOKOLIK, I. N. and TOON, O. B. "Incorporation of mineralogical composition into models of the radiative properties of mineral aerosol from UV to IR wavelengths." Journal of Geophysical Research 104 (1999): 9423-9444. doi: 0148-0227/99/1998JD20004850.
SWAP, R. et al. "Saharan dust in the Amazon Basin." Tellus 44B (1992): 133-149. doi: 10.1034/j.1600-0889.1992.t01-1-00005.x.
TALBOT, R. W. et al. "Aerosol Chemistry During the Wet Season in Central Amazonia: The Influence of Long-Range Transport." Journal of Geophysical Research 95 (1990): 16955-16969. 0148-0227/90/90JD-00639.
TAYLOR, M. et al. "Global aerosol mixtures and their multiyear and seasonal characteristics." Atmospheric Environment 116 (2015): 112-129. doi: 10.1016/j.atmosenv.2015.06.029.
TOLEDANDO, C. et al. "Airmass Classification and Analysis of Aerosol Types at El Arenosillo (Spain)." Journal of Applied Meteorology and Climatology 48 (2009): 962-981. doi: 10.1002/qj.54.
VALENZUELA, A. et al. "Aerosol properties retrieved from sky radiance at the Principal Plane for nonspherical particles." IV Reunión Española de Ciencia y Tecnología del Aerosol - RECTA 2010 (2010):1-6.
WANG, H. et al. "Comparison of climate response to anthropogenic aerosol versus greenhouse gas forcing: Distinct patterns." Journal of Climate 29 (2016): 5175-5188. doi:10.1175/jcli-d-16-0106.